the FEBS Journal

Activation loop 3 and the 170 loop interact in the active conformation of coagulation factor VIIa

Egon Persson and Ole H. Olsen

Haemostasis Biochemistry, Novo Nordisk A/S, Novo Nordisk Park, Måløv, Denmark

Keywords
activation loop; allosteric activation; factor VIIa; initiation of coagulation; tissue factor

Correspondence
E. Persson, Haemostasis Biochemistry, Novo Nordisk A/S, Novo Nordisk Park, G8.2.76, DK-2760 Måløv, Denmark
Fax: +45 4466 3450
Tel: +45 4443 4351
E-mail: egpe@novonordisk.com

(Received 3 December 2008, revised 20 March 2009, accepted 30 March 2009)

doi:10.1111/j.1742-4658.2009.07028.x

The initiation of blood coagulation involves tissue factor (TF)-induced allosteric activation of factor VIIa (FVIIa), which circulates in a zymogen-like state. In addition, the (most) active conformation of FVIIa presumably relies on a number of intramolecular interactions. We have characterized the role of Gly372(223) in FVIIa, which is the sole residue in activation loop 3 that is capable of forming backbone hydrogen bonds with the unusually long 170 loop and with activation loop 2, by studying the effects of replacement with Ala [G372(223)A]. G372A-FVIIa, both in the free and TF-bound form, exhibited reduced cleavage of factor X (FX) and of peptidyl substrates, and had increased K_m values compared with wild-type FVIIa. Inhibition of G372A-FVIIa·sTF by *p*-aminobenzamidine was characterized by a seven-fold higher K_i than obtained with FVIIa·sTF. Crystallographic and modelling data suggest that the most active conformation of FVIIa depends on the backbone hydrogen bond between Gly372(223) and Arg315(170C) in the 170 loop. Despite the reduced activity and inhibitor susceptibility, native and active site-inhibited G372A-FVIIa bound sTF with the same affinity as the corresponding forms of FVIIa, and burial of the N-terminus of the protease domain increased similarly upon sTF binding to G372A-FVIIa and FVIIa. Thus Gly372(223) in FVIIa appears to play a critical role in maturation of the S1 pocket and adjacent subsites, but does not appear to be of importance for TF binding and the ensuing allostery.

The low intrinsic enzymatic activity and membrane affinity of blood coagulation factor VIIa (FVIIa) allow it to circulate in a quiescent state, but at the same time being endoproteolytically pre-activated and poised to initiate blood coagulation upon exposure to tissue factor (TF). Binding to TF is required for the membrane-associated procoagulant activity that triggers the clotting cascade [1,2]. Importantly, formation of the binary complex localizes FVIIa to the site of vascular damage, positions the active site at an appropriate distance above the cell surface [3], and induces allosteric stimulation of FVIIa [4], all of which contribute to a dramatic enhancement of factor IX and X (FX) activation.

Free FVIIa exists primarily in the zymogen-like conformation. TF binding is required for its biological activity, and the mechanism of TF-induced allosteric stimulation of FVIIa remains a subject of research. Available crystal structures of free [5–8] and TF-bound FVIIa [9–11] lack conspicuous structural differences, primarily due to the presence of active site inhibitors. In one of the structures of free FVIIa [8], the inhibitor was even allowed to diffuse out of the active site, but, probably due to crystal constraints, only small structural alterations, including the S1 pocket, were observed. The structures can thus be used to identify amino acid residues that provide contacts between the two proteins, and Met306(164) in FVIIa (the

Abbreviations
fFR-cmk, D-Phe-Phe-Arg-chloromethyl ketone; FVII(a), (activated) factor VII; FX(a), (activated) factor X; HX, hydrogen exchange; mPEG-ButyrALD-2000, methoxypolyethyleneglycol-butyraldehyde with an average molecular weight of 2000; PABA, *p*-aminobenzamidine; (s)TF, (soluble) tissue factor.

chymotrypsinogen numbering is indicated in parentheses) is the key contact point with TF [9–12]. A number of loss-of-function mutations were identified in an alanine scanning mutagenesis study of FVIIa, shedding light on the amino acid residues that are important for TF binding and/or the cofactor effect [13]. In terms of intramolecular propagation of the TF-induced signal, the most interesting mutations are those that only affect activity of the FVIIa·TF complex.

The amino acid residues that determine the zymogenicity of free FVIIa are as interesting as those involved in the TF-induced allostery. Amino acid residues in FVIIa that are involved in the conformational balance that governs the equilibrium between zymogen-like and active conformations, which is strongly in favour of the former, can be identified by gain-of-activity mutations. Site-directed mutagenesis at certain positions in FVIIa has indeed resulted in molecules with increased intrinsic activity, and pinpointed amino acid residues that potentially serve as zymogenicity determinants. The most dramatic enhancements of FX activation have been observed with FVIIa variants containing a Gln substitute for Met298(156), especially when combined with replacements at positions 158(21) and 296(154) [14–17]. The high specific activity of these FVIIa variants is presumably linked to a more stable burial of the N-terminus of the protease domain in the activation pocket of the activation domain [15]. This event is (part of) the mechanism that TF employs to stimulate FVIIa [4,18]. Amino acid changes at a few other positions in FVIIa have also had a positive impact on the intrinsic activity [15,19,20]. However, the existing crystal structures do not suggest positions suitable for mutagenesis in order to create new FVIIa variants with higher activity.

An attractive FVIIa activation hypothesis was put forward based on the crystal structure of zymogen FVII in complex with an exosite-binding inhibitory peptide [21]. The authors proposed that FVIIa activation is accompanied by a three-residue β strand re-registration that allows the N-terminus to engage in a critical salt bridge with Asp343(194). However, the involvement of β-strand re-registration in the TF-induced allosteric effect on FVIIa was challenged when intermolecular crystal contacts were found at this very site [22]. Moreover, one study [23] has shown that introduction of a disulfide bond into FVIIa to lock the β strands in the active conformation can yield variants with enhanced intrinsic amidolytic (but not proteolytic) activity, whereas another study failed to prove a positive effect of trapping active FVIIa [24].

The difficulties in crystallizing free, uninhibited FVIIa have prompted us to search for an alternative structure-based source of input for structure–function studies aimed at unveiling the regulators of FVIIa zymogenicity and elucidating the pathway of TF-induced allostery. In recent years, we have studied the solution structures of various forms of FVII(a) using hydrogen exchange mass spectrometry (HX-MS). As part of this endeavour, we set out to identify the conformational switch by which TF turns on FVIIa by comparing free and TF-bound FVIIa. We found a short stretch [residues 370–372(221–223)] of activation loop 3 located at a crossroads of the suggested TF-induced allosteric path that apparently plays a particularly interesting role [25,26]. The present report focuses on Gly372(223), which was not included in the comprehensive alanine scanning mutagenesis study of FVIIa [13]. This amino acid residue interacts with activation loop 2 and the 170 loop via backbone hydrogen bonds with Ser333(185) and Arg315(170C), respectively. The latter bond is unique to FVIIa, i.e. is not found in other chymotrypsin-like enzymes, was recently shown to be stabilized by TF [25], and may thus coincide with a need to restrict the flexibility of the unusually long 170 loop of FVIIa. It is also the only possible backbone interaction between activation loop 3 and the 170 loop. Hence the two hydrogen bonds involving Gly372(223) may indirectly stabilize the active site region (via the 170 loop) as well as the insertion of the N-terminal tail (via activation loop 2). This hypothesis has been scrutinized by mutating Gly372(223) to Ala, which, according to molecular modelling, should weaken or abolish the hydrogen bond to Arg315(170C). The data clearly indicate that a Gly residue at position 372(223), and the resulting two hydrogen bonds, is a prerequisite to attain the most active conformation of FVIIa but not in order to respond to TF.

Results

Determination of active concentrations

Titrations of G372A-FVIIa and FVIIa with D-Phe-Phe-Arg-chloromethyl ketone (fFR-cmk) were performed to determine the true concentrations of active enzyme, and to ensure that all comparisons of the two forms of FVIIa were performed using the concentrations of active enzyme. The enzymes were diluted to a concentration of 100 nM based on the measured absorbance of the stock solution at 280 nm. In agreement with this, G372A-FVIIa and FVIIa were both found to have an active concentration of about 105 nM according to the fFR-cmk titrations (data not shown). The concentrations used in all

functional tests were based on the results of the titration experiment.

Enzymatic activity, inhibitor reactivity and sTF binding of G372A-FVIIa

The very slow auto-activation of G372A-FVII, or rather the need to add factor IXa for activation to occur, was the first sign of the relatively low specific activity of free G372A-FVIIa. Indeed, G372A-FVIIa displayed decreased specific enzymatic activity compared with FVIIa for both small (S-2288) and macromolecular (FX) substrates. The cleavage of S-2288 and FX by free G372A-FVIIa occurred seven to eight times more slowly and with modestly increased K_m values compared with FVIIa (Table 1). In the presence of soluble TF (sTF, residues 1–219), S-2288 (2.2-fold) and FX (4.3-fold) were still processed at a reduced rate by G372A-FVIIa, and K_m for S-2288 was increased by a factor of four (Fig. 1A). Results obtained with S-2366 also revealed a reduced hydrolysis rate and an increased K_m value (Fig. 1B). Use of two other chromogenic substrates, S-2238 and S-2765, confirmed the suboptimal activity of G372A-FVIIa bound to sTF, but estimation of the kinetic constants was not possible (Fig. 1C,D). A five-fold higher concentration of G372A-FVIIa was required in all these experiments to obtain similar levels of amidolytic activity to those obtained with FVIIa. It should be kept in mind that sTF fully represents full-length TF in terms of the protein–protein interactions with FVIIa, and has the same ability to stimulate amidolytic activity. However, due to the lack of a transmembrane region, i.e. an inability to dramatically lower the K_m, it cannot exert the same dramatic impact on FX activation. When G372A-FVIIa was bound to lipidated TF, FX activation was only reduced by a factor of two, and the K_m was not significantly different from that of the wild-type complex. Hence, with G372A-FVIIa, we observed a simultaneous but not always parallel decrease in amidolytic and proteolytic activities. With regard to the catalytic efficiency, the overall functional defect of G372A-FVIIa was, if anything, smaller in the presence of TF, which suggests that the allosteric effect of TF, influencing burial of the N-terminus, and the extent of catalytic stimulation by TF are not attenuated by the G372A mutation. However, the more pronounced difference in affinity for the peptidyl substrates, especially S-2288 and S-2238, between wild-type and G372A-FVIIa in the presence of sTF suggests that the mutation precludes efficient cofactor-induced maturation of substrate subsites (S1–S3). In line with a less mature S1 pocket in G372A-FVIIa, especially when bound to sTF, the K_i value for inhibition by *p*-aminobenzamidine (PABA) was seven-fold higher for G372A-FVIIa in complex with sTF than for sTF-bound FVIIa (0.70 versus 0.10 mM) (Fig. 2).

The kinetics of sTF binding as measured by surface plasmon resonance were found to be very similar for G372A-FVIIa and FVIIa (Fig. 3). The association and dissociation rate constants and the derived equilibrium dissociation constant were 2.4×10^5 $M^{-1}\cdot s^{-1}$, $1.5 \times 10^{-3}\cdot s^{-1}$ and 6.2 nM, respectively, for G372A-FVIIa. The corresponding values for FVIIa were 2.5×10^5 $M^{-1}\cdot s^{-1}$, $1.3 \times 10^{-3}\cdot s^{-1}$ and 5.2 nM, respectively. Moreover, incorporation of the active site inhibitor fFR-cmk had identical effects on the sTF binding kinetics of G372A-FVIIa and wild-type FVIIa (data not shown), primarily manifested by a 2.5-fold decrease in the dissociation rate, which is in agreement with what has been observed previously with FVIIa [27].

Accessibility of the terminal amino group of the protease domain

The susceptibility of the N-terminus to chemical modification, which is detrimental to FVIIa activity, reflects its solvent exposure. The relative degree of exposure was probed using a low-molecular-weight reagent

Table 1. Kinetic constants for hydrolysis of S-2288 and activation of FX by G372A-FVIIa and FVIIa. Values are means ± standard deviation.

	FX			S-2288	
Enzyme	k_{cat} ($\times 10^{-6}$ s^{-1})	K_m (μM)	k_{cat}/K_m ($M^{-1}\cdot s^{-1}$)	v_{max} ($mOD\cdot min^{-1}$ nM^{-1})	K_m (mM)
G372A-FVIIa	7 ± 2	5.4 ± 1.1	1.3	0.098 ± 0.006	14 ± 1
FVIIa	49 ± 10	3.0 ± 0.4	16	0.79 ± 0.05	10 ± 1
G372A-FVIIa·sTF	620 ± 90	3.2 ± 0.7	190	2.2 ± 0.1	7.1 ± 1.0
FVIIa·sTF	2700 ± 500	1.9 ± 0.5	1400	4.9 ± 0.2	1.8 ± 0.2
G372A-FVIIa·lipTF	2100 ± 200	0.012 ± 0.002	180 000		
FVIIa·lipTF	4000 ± 300	0.015 ± 0.002	270 000		

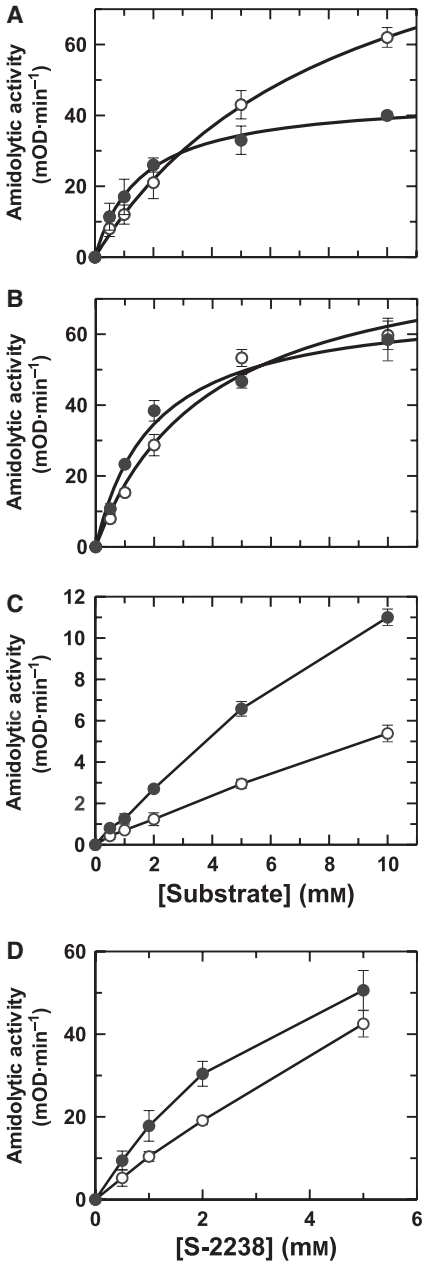

Fig. 1. Peptidyl substrate hydrolysis by G372A-FVIIa (50 nM) and FVIIa (10 nM) bound to sTF. The rates of cleavage (mean ± SD, $n = 3$) of four different substrates by mutant (○) and wild-type FVIIa (●) are shown. The data obtained with S-2288 and S-2366 were fitted to the Michaelis–Menten equation, and non-linear regression (using GraFit) was used to derive the kinetic constants. (A) Substrate S-2288. v_{max} and K_m values for G372A-FVIIa were 2.2 mOD·min^{-1}·nM^{-1} and 7.1 mM and those for for FVIIa were 4.9 mOD·min^{-1}·nM^{-1} and 1.8 mM; (B) Substrate S-2366. v_{max} and K_m values for G372A-FVIIa were 1.7 mOD·min^{-1}·nM^{-1} and 3.9 mM and those for FVIIa were 6.9 mOD·min^{-1}·nM^{-1} and 1.9 mM; (C) Substrate S-2765. v_{max} and K_m values were not estimated; (D) Substrate S-2238. v_{max} and K_m values were not estimated. Due to solubility problems, the highest final concentration of S-2238 was 5 mM.

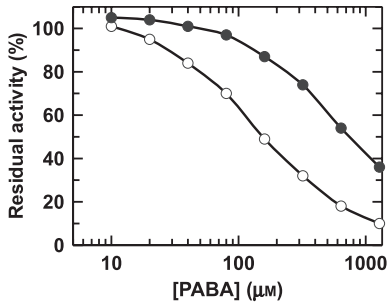

Fig. 2. PABA inhibition of G372A-FVIIa and FVIIa bound to sTF. The residual amidolytic activity of G372A-FVIIa (●) and FVIIa (○), saturated with sTF, when at equilibrium with the indicated PABA concentrations is shown. The data yielded K_i values of 0.70 mM for G372A-FVIIa·sTF and 0.10 mM for FVIIa·sTF.

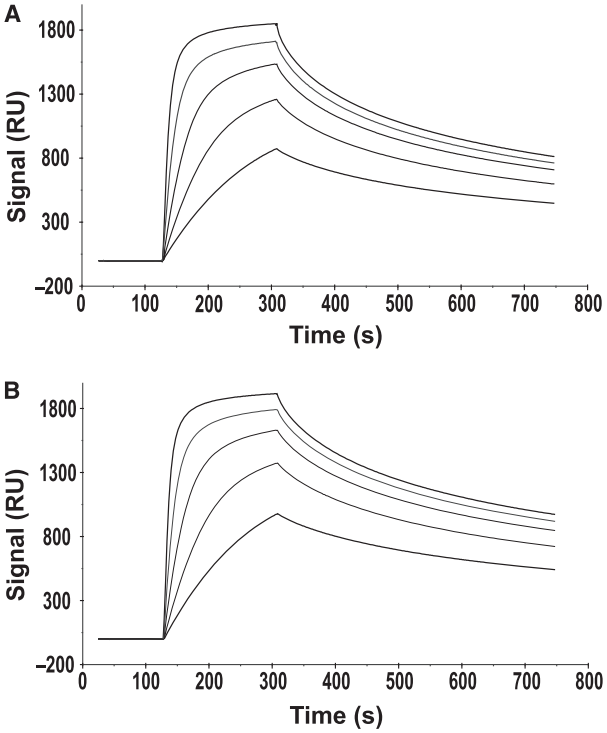

Fig. 3. Kinetics of G372A-FVIIa and FVIIa binding to immobilized sTF measured by surface plasmon resonance. Corrected sensorgrams are shown for the interactions between G372A-FVIIa (A) and FVIIa (B) with sTF. The curves represent analyte injected at 20, 40, 80, 160 and 320 nM, respectively, from bottom to top.

(potassium cyanate; KNCO), whose effect can be measured as disappearance of enzymatic activity, and with a much larger, slow-reacting reagent (mPEG-Butyr-ALD-2000, i.e. methoxypolyethyleneglycol-butyraldehyde with an average MW of 2000) which allows visualization of the modification using SDS–PAGE. The rate of carbamylation of the N-terminal amino group [Ile153(16)] of the protease domain in G372A-

FVIIa was indistinguishable from that of FVIIa in both the free form and in complex with sTF. G372A-FVIIa and FVIIa lost 17–18% activity per 10 min of incubation with KNCO, retaining 30–35% activity after 1 h. G372A-FVIIa·sTF and FVIIa·sTF lost around 7% activity per 10 min, and retained about 65% activity after 1 h. We then applied the technique of N-terminal pegylation to visualize the relative solvent exposure of the N-terminus of FVIIa. To the best of our knowledge, this is the first time that this technique has been applied for this purpose. As shown in Fig. 4A, the free forms of G372A-FVIIa and FVIIa were more rapidly pegylated than their sTF-bound counterparts. Importantly, when the intensity of the band representing monopegylated FVIIa (FVIIa-PEG_{2k}) was plotted as a function of time, a similar protective effect of sTF was observed for G372A-FVIIa and FVIIa (Fig. 4B). The apparent difference in the rate of pegylation of the free forms is not significant over several experiments. Pegylation, presumably also N-terminal, of sTF was also observed, but this

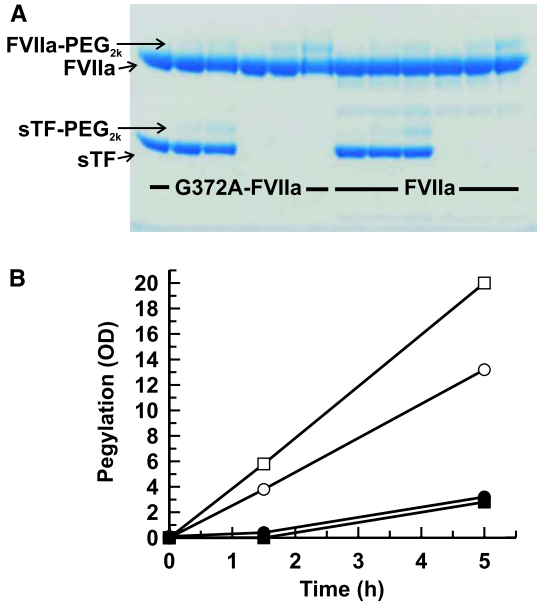

Fig. 4. N-terminal pegylation of G372A-FVIIa and FVIIa. (A) Pegylation of free and TF-bound G372A-FVIIa and FVIIa visualized by SDS–PAGE. At each time point, a 12 μL aliquot of the reaction mixture was removed, added to sample buffer, applied to the gel and run under non-reducing conditions. The samples, from left to right, are G372A-FVIIa/sTF, G372A-FVIIa, FVIIa/sTF and FVIIa analysed at time zero and after 1.5 and 5 h of pegylation, respectively. The positions of the bands representing pegylated FVIIa (FVIIa-PEG2k), pegylated sTF (sTF-PEG2k) and the unmodified proteins are denoted by arrows. (B) Time course of pegylation. The amounts of pegylated FVIIa (○, ●) and G372A-FVIIa (□, ■) in the absence (open symbols) and presence of sTF (closed symbols) were quantified by densitometric analysis of the gel shown in (A).

probably has no impact on the ability of sTF to bind FVIIa, based on the FVIIa–sTF crystal structure [9]. Under all circumstances, the presence of sTF protected the N-terminus of the protease domain from modification. In a control experiment, no pegylation of zymogen FVII (R152A-FVII), i.e. of the N-terminus of the γ-carboxyglutamic acid-rich domain (light chain) or of surface-exposed lysine residues in FVII, was observed, confirming that only the protease domain N-terminus was targeted (not shown).

Structural analyses and modelling

The presence of the unique hydrogen bond in FVIIa between Gly372(223) and Arg315(170C) (Fig. 5A) prompted us to examine the local structure of homologous proteases with other residues in the position corresponding to 372(223). The conformations of activation loop 3 of trypsin (Protein Data Bank accession number 1tgt) and trypsinogen (Protein Data Bank accession number 1j8a) with Asn in this position, albeit with Φ,Ψ angles far from the allowed Ramachandran region, are virtually identical to that of FVIIa. Modelling of Ala372(223) into FVIIa showed that the Cβ atom clashed with that of Arg315(170C), and energy minimization weakened the backbone hydrogen bond between the two residues (Fig. 5B). However, the hydrogen bond with Ser333(185) appeared to be preserved. Our modelling findings are in agreement with the experimental data, showing reduced enzymatic activity and S1 pocket maturation but at the same time an unaltered conformational distribution of the N-terminal tail and a normal response to TF.

Discussion

FVIIa contains the canonical activation domain characteristic of proteases in the trypsin family [28,29]. However, FVIIa differs from its relatives in that the activation domain does not spontaneously mature upon endoproteolytic generation of a protease domain N-terminus, and requires cofactor (TF) binding to accomplish the transition. Mutagenesis studies have shown that FVIIa is allosterically regulated by conformational linkages involving the TF-interactive region of the protease domain, the catalytic cleft and the macromolecular substrate exosite (including the activation pocket) [4]. A previous HX-MS study of the solution structure of FVIIa showed that activation loop 3 is one of the regions that is influenced by sTF binding [25]. Subsequent work, including molecular dynamics simulations, pinpointed in particular the C-terminal part of activation loop 3 [26]. More precisely, an

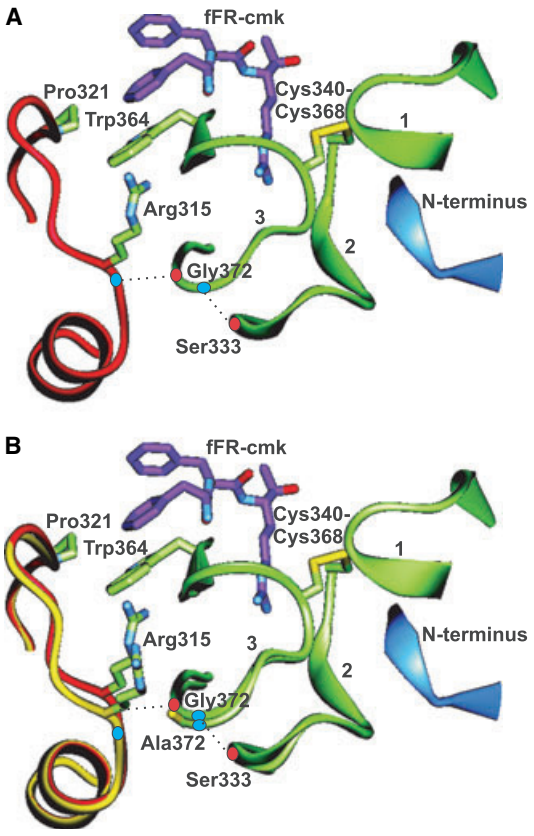

Fig. 5. Structure of FVIIa and model of G372A-FVIIa. (A) Energy-minimized structure of FVIIa. Representation of the part of FVIIa discussed in the text (based on Protein Data Bank accession number 1dan [9]), encompassing the N-terminal tail (blue), activation loops 1–3 (green), the TF-interactive helix and the 170 loop (red), and the covalently attached inhibitor fFR-cmk (purple). The hydrogen bonds from Gly372(223) to Arg315(170C) and Ser-333(185) are indicated by dotted lines, with backbone carbonyls and amides in red and blue, respectively; (B) Overlay of the energy-minimized FVIIa structure and the energy-minimized model of G372A-FVIIa. The C_β atom of the Ala residue introduced at position 372(223) clashes with the C_β of Arg315(170C), resulting in a weakened, or possibly abrogated, hydrogen bond and repositioning of the 170 loop (yellow).

amide hydrogen within residues 370–372(221–223), most likely that of Gly372(223), was fully exposed in free FVIIa (representing the latent, zymogen-like conformation) and engaged in a hydrogen bond in TF-bound FVIIa (the active conformation). Our model suggests that the backbone amide of Gly372(223) participates in a hydrogen bond with the backbone carbonyl of Ser333(185), thus connecting activation loops 2 and 3 in the active conformation (Fig. 5A) [26]. In addition, the backbone carbonyl of Gly372(223) hydrogen bonds to the backbone amide of Arg315(170C). By comparing HX-MS data obtained with peptides 314–325(170B–178) and 312–325(170–178), it can be inferred that the Gly372(223)–Arg315(170C) hydrogen bond exists both in free and TF-bound FVIIa, and that it is more stable in the presence of TF (Online Supplemental Data to [25]). We propose that this region and its interactions play a pivotal role in the physiologically relevant, TF-induced allosteric effects on FVIIa or are important in order to attain the most active conformation of FVIIa. According to our hypothesis, the hydrogen bond between Gly372(223) and Arg315(170), observed in structures of FVIIa bound to TF, participates in stabilization of the 170 loop. This should have a positive impact on the substrate binding cleft. A need to restrict the 170 loop to achieve full enzymatic activity is supported by the positive effect of grafting of the corresponding (shorter) loop from trypsin, which has a proline residue at the apex, into FVIIa, although a simple truncation was of no benefit [30]. The other hydrogen bond, with Ser333(185), connects activation loops 2 and 3 and supports the activation domain by stabilizing Ala369(221A) and the Cys340(191)–Cys368(220) disulfide. This should facilitate insertion of the N-terminal tail into the activation pocket. Hence the presence of TF stabilizes the two hydrogen bonds, i.e. it indirectly supports the substrate binding cleft and correct insertion of the N-terminal tail into the activation pocket. To assess this hypothesis, we mutated Gly372(223) to Ala, a substitution that was not included in the published alanine scanning mutagenesis study of FVIIa [13], and investigated the effects of the mutation on the enzymatic maturation of FVIIa and on the response of FVIIa to TF.

Our measurements, in both the presence and absence of TF, revealed that the amidolytic and proteolytic activities of G372A-FVIIa were reduced compared with FVIIa. In accordance with the lower specific activity, G372A-FVIIa exhibited decreased inhibitor susceptibility, and the data obtained with PABA (and peptidyl substrates) indicated an immature S1 pocket. This may lead to positioning of the substrate P1 Arg residue that is incompatible with efficient cleavage of the scissile bond. This would affect FX and peptide hydrolysis similarly, supported by the similar decrease in the rate of cleavage of both types of substrates. The effect of the G372(223)A mutation on K_m is more conspicuous with peptidyl substrates than with FX, indicating that substrate subsites located in the vicinity of the active site and sensed by the peptidyl substrate are influenced, in contrast to the remote exosites, e.g. in the vicinity of the activation pocket, that affect FX binding, which are only affected to a very small extent, if at all [31–33]. The effects on the S1–S3 subsites, of

which S2 and S3 primarily determine the affinity for the small chromogenic substrates, may result in suboptimal orientation of the P1 Arg residue. The magnitude of the effects of the G372(223)A mutation is slightly substrate-dependent. The fact that the relative reduction in activity was not greater in the presence of cofactor strongly suggests that the allosteric mechanism behind the TF-induced activity enhancement is intact in G372A-FVIIa. It also suggests that the G372(223)A mutation results in loss of an intramolecular bond from the FVIIa molecule that is present in the active conformation of both the free and TF-bound form, rather than shifting the equilibrium between the zymogen-like and active conformations, and is in agreement with the HX-MS data [25]. Functional TF-induced allostery is supported by the ability of sTF to facilitate insertion of the N-terminal tail of G372A-FVIIa into the activation pocket to the same extent as with wild-type FVIIa. Finally, sTF bound both variants with the same affinity, and incorporation of an active site inhibitor into FVIIa and G372A-FVIIa increased the affinity for sTF in an indistinguishable manner. The differences and similarities between G372A-FVIIa and FVIIa seen in complex with sTF are presumably also exist for full-length TF because the soluble form retains the entire extracellular domain of TF and its binding interface with FVIIa. Thus the functional defects of G372A-FVIIa and any differences from FVIIa, whether free or bound to TF, appear to be confined to the substrate binding cleft (the 170 loop) in the active site region and the S1 pocket, whereas the intramolecular connections, for instance between the TF-binding region and the active site and between the TF-binding region and the activation domain, appear to function normally.

In order to further elucidate the effects of the G372(223)A mutation, we analysed the mutation *in silico*. The resulting model showed that the introduced C_β atom exhibited close contact with that of Arg315(170C), thus abrogating or weakening the main-chain hydrogen bond between these two residues (Fig. 5B). In contrast, the hydrogen bond to Ser333(185) was preserved. This is in agreement with our experimental findings, which showed reduced enzymatic activity but at the same time an unaltered conformational distribution of the N-terminal tail and a normal response to TF. Hence, the observation of a compromised hydrogen bond in the model again suggests that this bond is important in order to attain the most active conformation of FVIIa but not for allosteric regulation of FVIIa by TF.

In recent years, a number of crystal structures have demonstrated some conformational plasticity of FVIIa, especially in the vicinity of the S1 pocket [11,34], in the first part of activation loop 3, and in the area of the TF-interactive helix and the 170 loop [8,35], areas that are stabilized by TF [9,25,26]. The Lys341(192)–Gly342(193) peptide bond, which constitutes part of the oxyanion hole and the rim of the S1 pocket, may rotate 180 °C depending on the type of inhibitor bound. Similarly, rotation of the Ser363(214)–Trp364(215) peptide bond and perturbation of the Cys340(191)–Cys368(220) disulfide bridge, also forming part of the S1 pocket, are observed when benzamidine is soaked out of FVIIa [8]. Thus the classical activation loop 3 [residues 365–372(216–223)] is not the only flexible element in the vicinity of the substrate binding cleft of FVIIa. This is further supported by the observation that the side chain of Trp364(215) moves closer to the S2 pocket, leading to rearrangement of residues 364–369(215–221A), as seen for a structure of FVIIa obtained in the presence of an indole-based inhibitor (Protein Data Bank accession number 2fb9) [34]. Altogether, these observations indicate a high degree of flexibility in this region of FVIIa. However, when benzamidine is soaked out of FVIIa, the resulting structure reveals a slightly rotated TF-interactive helix that in turn abrogates the Gly372(223)–Arg315(170C) hydrogen bond and leads to a disordered 170 loop (Protein Data Bank accession numbers 1kli and 1klj) [8]. Thus there is a similarly larger conformational flexibility in this region in the absence of inhibitor (Fig. 6). Nevertheless, the

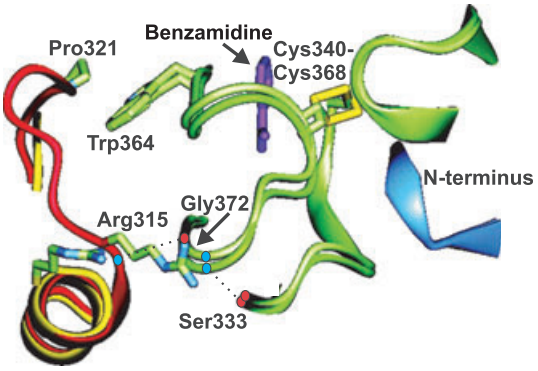

Fig. 6. Comparison of FVIIa structures with benzamidine in the S1 pocket and after the inhibitor has been soaked out. The structure with Protein Data Bank accession number 1kli [8] was used to produce the structure with benzamidine, with the TF-interactive helix and the 170 loop shown in red. The structure with Protein Data Bank accession number 1klj [8] was used to produce the structure with the free S1 pocket, with the helix and loop shown in yellow. In the absence of benzamidine, the 170 loop is more flexible (not visible in the structure), and consequently the hydrogen bond between Gly372(223) and Arg315(170C) is broken.

N-terminus remains inserted into the activation pocket regardless of whether benzamidine is present or has been soaked out. A reason for this is found by inspecting the crystal packing in the Protein Data Bank structures 1kli and 1klj. It shows close contacts between activation loop 1 and the C-terminal 399–404(250–255) loop of neighbouring molecules. The distance between the C_β atoms of Arg290(147) and Leu401(252) in neighbouring molecules is only 4 Å, possibly imposing rigidity on activation loop 1 and keeping the N-terminus in place. Hence, crystallographic structural data suggest that the 170 loop, in addition to being part of the substrate binding cleft, exerts a stabilizing effect on the rest of this cleft.

Our data suggest important roles for the hydrogen bonds of Gly372(223) in the active conformation of FVIIa, namely in stabilization of regions in the FVIIa molecule with documented flexibility that are involved in substrate processing. These bonds are two of the components of the invisible scaffold supporting the active conformation. One bond participates in stabilization of the 170 loop while the other connects activation loops 2 and 3. Weakening or abrogation of the former bond, as in G372A-FVIIa, results in a more flexible 170 loop (in both free and TF-bound FVIIa) and has a negative impact on the substrate binding cleft, as manifested by decreased enzymatic activity and inhibitor susceptibility.

Experimental procedures

Materials and standard methods

Recombinant wild-type FVIIa and sTF were prepared as described previously [36,37]. Their concentrations were determined by absorbance measurements at 280 nm using absorption coefficients of 1.32 and 1.5, respectively, for a 1 mg·mL^{-1} solution and MW of 50 000 and 25 000, respectively. R152A-FVII was a gift from H. R. Stennicke (Novo Nordisk A/S, Bagsværd, Denmark). FX, FXa and factor IXaβ were obtained from Enzyme Research Laboratories (South Bend, IN, USA). The chromogenic *p*-nitroanilide substrates S-2288 (D-Ile-Pro-Arg-pNA), S-2366 (pyroGlu-Pro-Arg-pNA), S-2238 (D-Phe-pipecolyl-Arg-pNA) and S-2765 (benzyloxycarbonyl-D-Arg-Gly-Arg-pNA) were purchased from Chromogenix (Milan, Italy). The active-site inhibitor D-Phe-Phe-Arg-chloromethyl ketone (fFR-cmk) was purchased from Bachem (Bubendorf, Switzerland), *p*-aminobenzamidine (PABA) and sodium cyanoborohydride ($NaCNBH_3$) from Sigma-Aldrich (St Louis, MO, USA), methoxypolyethyleneglycol-butyraldehyde 2000 (mPEG-ButyrALD-2000) from Nektar Therapeutics (Huntsville, AL, USA) and potassium cyanate (KNCO) from Fluka (Buchs, Switzerland).

Mutagenesis and isolation of G372A-FVIIa

The alanine substitution for glycine at position 372(223) in FVII was introduced using a QuikChange kit (Stratagene, La Jolla, CA, USA) and the human FVII expression plasmid pLN174 [38]. The sense primer 5′-GGCTGCGCAAC CGTG***GCC***CACTTTGGGG-3′ and a complementary reverse primer were used (base substitution in bold italic and the altered codon underlined). The plasmid was prepared using a QIAfilter plasmid midi kit (Qiagen, Valencia, CA, USA). The coding sequence of the entire protease domain was verified to exclude the presence of additional mutations. Baby hamster kidney cell transfection and selection, as well as expression and purification of G372A-FVII, were performed as described previously [12,15]. G372A-FVII was activated by incubation with factor IXaβ (10% w/w) at 37 °C overnight, followed by chromatography on an F1A2 (anti-FVIIa) immunoaffinity column.

Active site titration

G372A-FVIIa and FVIIa (100 nM) were incubated with sTF (500 nM) and fFR-cmk (0–120 nM) in 50 mM Hepes, pH 7.4, containing 0.1 M NaCl, 5 mM $CaCl_2$ and 0.01% v/v Tween-80, overnight at room temperature. An aliquot (20 μL) of the incubation mixture was then incubated with 1 mM S-2288 (total volume 200 μL) in the same buffer to determine residual activity. The absorbance was continuously monitored at 405 nm using a kinetic microplate reader (SpectraMax 190; Molecular Devices, Sunnyvale, CA, USA).

Activity measurements

All assays were performed in 50 mM Hepes, pH 7.4, containing 0.1 M NaCl, 5 mM $CaCl_2$ and 1 mg·mL^{-1} bovine serum albumin and monitored as described above. The amidolytic activity of G372A-FVIIa and FVIIa was measured by incubating G372A-FVIIa (500 nM free or 50 nM plus 150 nM sTF) and FVIIa (100 nM free or 10 nM plus 150 nM sTF) with 0.5–10 mM chromogenic substrate (total volume 100 μL). The proteolytic activity of G372A-FVIIa and FVIIa was measured by incubating G372A-FVIIa (500 nM free, 5 nM plus 150 nM sTF, or 1 nM plus 1 pM lipidated TF) and FVIIa (100 nM free, 1 nM plus 150 nM sTF, or 1 nM plus 1 pM lipidated TF) with 0.1–10 μM FX (free enzyme and in the presence of sTF) or 5–320 nM FX (in the presence of lipidated TF) for 20 min. The reaction was terminated using excess EDTA, and the FXa activity was measured by adding S-2765 (final concentration 0.5 mM). After correction for background amidolytic activity of the FX preparation and of the FVIIa·sTF complexes, the FXa activity was converted to [FXa] using a FXa standard curve from 0.5 to 3 nM.

Inhibition by PABA

All reagents were diluted in the activity assay buffer described above. G372A-FVIIa (50 nM) and FVIIa (10 nM) in the presence of 150 nM sTF were incubated with 10–1280 μM PABA for 5 min prior to the addition of 1 mM S-2288 to measure the amount of residual uninhibited enzyme. The total assay volume was 100 μL. To calculate the K_i values for PABA inhibition using the expression $K_i = IC_{50}/(1 + [S]/K_m)$, K_m values for S-2288 of 7.1 and 1.8 mM were used for G372A-FVIIa·sTF and FVIIa·sTF, respectively [20].

Surface plasmon resonance measurements

Immobilization of sTF (1900 resonance units) on a research-grade CM5 sensor chip in a Biacore 3000 instrument (Biacore AB, Uppsala, Sweden) was performed using amine coupling chemistry by injecting 35 μL of a 25 $\mu g \cdot mL^{-1}$ solution of sTF in 10 mM sodium acetate, pH 3.0. G372A-FVIIa and FVIIa, in two-fold dilutions from 20 to 320 nM in 20 mM Hepes, pH 7.4, containing 0.1 M NaCl, 2 mM $CaCl_2$ and 0.005% surfactant P20, were injected at a flow rate of 20 $\mu L \cdot min^{-1}$. The association and dissociation phases were 3 and 10 min, respectively. To assess the effect of active site inhibitor incorporation on sTF binding kinetics, native and fFR-cmk-inhibited G372A-FVIIa and FVIIa were injected at a single concentration of 50 nM. The sTF-coated surface was regenerated between runs using a 90 s pulse of 50 mM EDTA, pH 7.4, at a flow rate of 20 $\mu L \cdot min^{-1}$. The kinetic parameters were calculated by global fitting of binding data to a 1 : 1 model using the software Biaevaluation 4.1 supplied by the manufacturer (Biacore AB).

N-terminal pegylation and carbamylation

In the pegylation experiments, G372A-FVIIa and FVIIa at a concentration of 10 μM, alone or after a 5 min preincubation with sTF (12 μM), were incubated with 2 mM mPEG-ButyrALD-2000 and 2 mM $NaCNBH_3$ in 50 mM Hepes, pH 7.4, containing 0.1 M NaCl and 5 mM $CaCl_2$. Samples were withdrawn before initiation of the reaction and after 1.5 and 5 h, and subjected to SDS–PAGE on a 10% NuPAGE Novex Bis/Tris gel (Invitrogen, Carlsbad, CA, USA). A control experiment was performed with 6.8 μM zymogen FVII (R152A-FVII). The intensities of the bands representing FVIIa-PEG_{2k} were quantified by transluminination using an AutoChemiSystem AC1 auto darkroom (UVP Inc., Upland, CA, USA). Carbamylation was carried out in the same buffer by incubating 2 μM G372A-FVIIa, 1 μM FVIIa, 500 nM G372A-FVIIa plus 1 μM sTF, and 100 nM FVIIa plus 200 nM sTF with 0.2 M KNCO. After 30 and 60 min, samples were withdrawn, diluted in buffer containing 1 $mg \cdot ml^{-1}$ bovine serum albumin, and the residual amidolytic activity was measured using the substrate S-2288 as previously described [15].

Structural analyses and molecular modelling

Analyses were performed within the frameworks of the molecular modeling package Quanta 2000 and the molecular mechanics force field CHARMm 27 (Accelrys Inc., San Diego, CA, USA). The model of G372A-FVIIa was created by mutating the side chain in FVIIa taken from the FVIIa·TF structure [9] (Protein Data Bank accession number 1dan) using the mutation facility within the protein modeling module in Quanta 2000, followed by energy minimization (250 steps of conjugated gradient in CHARMm).

Acknowledgements

We thank Anette Østergaard for excellent technical assistance and Dr Henning R. Stennicke for providing R152A-FVII (Novo Nordisk A/S, Novo Nordisk Park, Måløv, Denmark).

References

1 Davie EW, Fujikawa K & Kisiel W (1991) The coagulation cascade: initiation, maintenance and regulation. *Biochemistry* **30**, 10363–10370.
2 Kalafatis M, Swords NA, Rand MD & Mann KG (1994) Membrane-dependent reactions in blood coagulation: role of the vitamin K-dependent enzyme complexes. *Biochim Biophys Acta* **1227**, 113–129.
3 McCallum CD, Hapak RC, Neuenschwander PF, Morrissey JH & Johnson AE (1996) The location of the active site of blood coagulation factor VIIa above the membrane surface and its reorientation upon association with tissue factor. A fluorescence energy transfer study. *J Biol Chem* **271**, 28168–28175.
4 Ruf W & Dickinson CD (1998) Allosteric regulation of the cofactor-dependent serine protease coagulation factor VIIa. *Trends Cardiovasc Med* **8**, 350–356.
5 Pike ACW, Brzozowski AM, Roberts SM, Olsen OH & Persson E (1999) Structure of human factor VIIa and its implications for the triggering of blood coagulation. *Proc Natl Acad Sci USA* **96**, 8925–8930.
6 Kemball-Cook G, Johnson DJD, Tuddenham EGD & Harlos K (1999) Crystal structure of active site-inhibited human coagulation factor VIIa (des-Gla). *J Struct Biol* **127**, 213–223.
7 Dennis MS, Eigenbrot C, Skelton NJ, Ultsch MH, Santell L, Dwyer MA, O'Connell MP & Lazarus RA (2000) Peptide exosite inhibitors of factor VIIa as anticoagulants. *Nature* **404**, 465–470.

8 Sichler K, Banner DW, D'Arcy A, Hopfner KP, Huber R, Bode W, Kresse GB, Kopetzki E & Brandstetter H (2002) Crystal structures of uninhibited factor VIIa link its cofactor and substrate-assisted activation to specific interactions. *J Mol Biol* **322**, 591–603.
9 Banner DW, D'Arcy A, Chène C, Winkler FK, Guha A, Konigsberg WH, Nemerson Y & Kirchhofer D (1996) The crystal structure of the complex of blood coagulation factor VIIa with soluble tissue factor. *Nature* **380**, 41–46.
10 Zhang E, St Charles R & Tulinsky A (1999) Structure of extracellular tissue factor complexed with factor VIIa inhibited with a BPTI mutant. *J Mol Biol* **285**, 2089–2104.
11 Bajaj SP, Schmidt AE, Agah S, Bajaj MS & Padmanabhan K (2006) High resolution structures of *p*-aminobenzamidine- and benzamidine–VIIa/soluble tissue factor. *J Biol Chem* **281**, 24873–24888.
12 Persson E, Nielsen LS & Olsen OH (2001) Substitution of aspartic acid for methionine-306 in factor VIIa abolishes the allosteric linkage between the active site and the binding interface with tissue factor. *Biochemistry* **40**, 3251–3256.
13 Dickinson CD, Kelly CR & Ruf W (1996) Identification of surface residues mediating tissue factor binding and catalytic function of the serine protease factor VIIa. *Proc Natl Acad Sci USA* **93**, 14379–14384.
14 Petrovan RJ & Ruf W (2001) Residue Met^{156} contributes to the labile enzyme conformation of coagulation factor VIIa. *J Biol Chem* **276**, 6616–6620.
15 Persson E, Kjalke M & Olsen OH (2001) Rational design of coagulation factor VIIa variants with substantially increased intrinsic activity. *Proc Natl Acad Sci USA* **98**, 13583–13588.
16 Petrovan RJ & Ruf W (2002) Role of zymogenicity-determining residues of coagulation factor VII/VIIa in cofactor interaction and macromolecular substrate recognition. *Biochemistry* **41**, 9302–9309.
17 Persson E & Olsen OH (2002) Assignment of molecular properties of a superactive coagulation factor VIIa variant to individual amino acid changes. *Eur J Biochem* **269**, 5950–5955.
18 Higashi S, Nishimura H, Aita K & Iwanaga S (1994) Identification of regions of bovine factor VII essential for binding to tissue factor. *J Biol Chem* **269**, 18891–18898.
19 Persson E, Bak H & Olsen OH (2001) Substitution of valine for leucine 305 in factor VIIa increases the intrinsic enzymatic activity. *J Biol Chem* **276**, 29195–29199.
20 Persson E, Bak H, Østergaard A & Olsen OH (2004) Augmented intrinsic activity of factor VIIa by replacement of residues 305, 314, 337 and 374: evidence of two unique mutational mechanisms of activity enhancement. *Biochem J* **379**, 497–503.
21 Eigenbrot C, Kirchhofer D, Dennis MS, Santell L, Lazarus RA, Stamos J & Ultsch MH (2001) The factor VII zymogen structure reveals reregistration of β strands during activation. *Structure* **9**, 627–636.
22 Perera L & Pedersen LG (2005) A reconsideration of the evidence for structural reorganization in FVII zymogen. *J Thromb Haemost* **3**, 1543–1545.
23 Maun HR, Eigenbrot C, Raab H, Arnott D, Phu L, Bullens S & Lazarus RA (2005) Disulfide locked variants of factor VIIa with a restricted β-strand conformation have enhanced enzymatic activity. *Protein Sci* **14**, 1171–1180.
24 Olsen OH, Nielsen PF & Persson E (2004) Prevention of β strand movement into a zymogen-like position does not confer higher activity to coagulation factor VIIa. *Biochemistry* **43**, 14096–14103.
25 Rand KD, Jørgensen TJD, Olsen OH, Persson E, Jensen ON, Stennicke HR & Andersen MD (2006) Allosteric activation of coagulation factor VIIa visualized by hydrogen exchange. *J Biol Chem* **281**, 23018–23024.
26 Olsen OH, Rand KD, Østergaard H & Persson E (2007) A combined structural dynamics approach identifies a putative switch in factor VIIa employed by tissue factor to initiate blood coagulation. *Protein Sci* **16**, 671–682.
27 Sørensen BB, Persson E, Freskgård P-O, Kjalke M, Ezban M, Williams T & Rao LVM (1997) Incorporation of an active site inhibitor in factor VIIa alters the affinity for tissue factor. *J Biol Chem* **272**, 11863–11868.
28 Fehlhammer H, Bode W & Huber R (1977) Crystal structure of bovine trypsinogen at 1.8 Å resolution. II. Crystallographic refinement, refined crystal structure and comparison with bovine trypsin. *J Mol Biol* **111**, 415–438.
29 Huber R & Bode W (1978) Structural basis of the activation and action of trypsin. *Acc Chem Res* **11**, 114–122.
30 Soejima K, Mizuguchi J, Yuguchi M, Nakagaki T, Higashi S & Iwanaga S (2001) Factor VIIa modified in the 170 loop shows enhanced catalytic activity but does not change the zymogen-like property. *J Biol Chem* **276**, 17229–17235.
31 Shobe J, Dickinson CD, Edgington TS & Ruf W (1999) Macromolecular substrate affinity for the tissue factor–factor VIIa complex is independent of scissile bond docking. *J Biol Chem* **274**, 24171–24175.
32 Baugh RJ, Dickinson CD, Ruf W & Krishnaswamy S (2000) Exosite interactions determine the affinity of factor X for the extrinsic Xase complex. *J Biol Chem* **275**, 28826–28833.
33 Krishnaswamy S (2005) Exosite-driven substrate specificity and function in coagulation. *J Thromb Haemost* **3**, 54–67.
34 Groebke Zbinden K, Obst-Sander U, Hilpert K, Kühne H, Banner DW, Böhm HJ, Stahl M, Ackermann J, Alig L, Weber L *et al.* (2005) Selective and orally bioavailable phenylglycine tissue factor/factor VIIa inhibitors. *Bioorg Med Chem Lett* **15**, 5344–5352.

35 Rai R, Kolesnikov A, Spengeler PA, Torkelson S, Ton T, Katz BA, Yu C, Hendrix J, Shrader WD, Stephens R *et al*. (2006) Discovery of novel heterocyclic factor VIIa inhibitors. *Bioorg Med Chem Lett* **16**, 2270–2273.

36 Thim L, Bjoern S, Christensen M, Nicolaisen EM, Lund-Hansen T, Pedersen A & Hedner U (1988) Amino acid sequence and posttranslational modifications of human factor VIIa from plasma and transfected baby hamster kidney cells. *Biochemistry* **27**, 7785–7793.

37 Freskgård P-O, Olsen OH & Persson E (1996) Structural changes in factor VIIa induced by Ca^{2+} and tissue factor studied using circular dichroism spectroscopy. *Protein Sci* **5**, 1531–1540.

38 Persson E & Nielsen LS (1996) Site-directed mutagenesis but not γ-carboxylation of Glu-35 in factor VIIa affects the association with tissue factor. *FEBS Lett* **385**, 241–243.